Commodity Price Risk in Phosphorus Recycling Investments

Abstract: There are optimistic targets for phosphorus recycling from waste streams to solve environmental and supply issues simultaneously. The recycling process requires high energy inputs, thus the joint distribution of (input) energy and (output) fertilizer commodity prices is a crucial determinant of the profitability of investing. We propose a methodology to model the investment risk and price dependencies using quantile vector autoregression and copulas. We find that price dynamics are not stable when gas prices are high. Moreover standard approaches overestimate investment risk. Finally, we find that phosphorus recycling investments are only profitable with substantial subsidies or savings on disposal expenditures.

Keywords: copula, investment analysis, phosphorus recycling, time series econometrics

Introduction

Phosphorus pollution has exceeded planetary boundaries (Richardson et al., 2023) and mineral phosphorus sources are scarce (Barbieri et al., 2022). Recovering phosphorus fertilizers from wastewater streams, has therefore become a top policy priority to close nutrient cycles (Tonini et al., 2019; Brownlie et al., 2021; Springmann et al., 2018). In addition, phosphorus recycling could enhance resilience by reducing the EU's dependence on imported fertilizers (Brownlie et al., 2023). However, two major obstacles hinder the establishment of recycling facilities (Uhlemann et al., 2024). Firstly, recycling processes often require significant energy inputs, creating a trade-off between greenhouse gas and phosphorus pollution reduction targets (Shi et al., 2021). Secondly, investment in recycling facilities carries substantial risks, primarily driven by fluctuations in phosphorus and energy prices. Previous research indicates that phosphorus recycling from wastewater becomes viable for dairy processing organizations when phosphorus prices are high and energy prices are low (Uhlemann et al., 2024). Nevertheless, the European Union is determined to achieve a target of substituting 17 % of the phosphorus supply with recycled phosphorus (European Commission, 2020). Therefore, understanding the likelihood of these opposing price trends occurring together is crucial for evaluating the feasibility of recycling technologies in addressing phosphorus pollution and informing policy incentives for their adoption.

In this paper, we estimate the profitability and risk therein of investing in phosphorus recycling facilities from wastewater streams. We use the example of phosphorus rich dairy wastewater and develop a methodology to put a particular emphasis on the joint distribution and the dynamics of the marginal distribution of phosphorus and energy prices. More specifically, we use a copula approach and Quantile Vector Autoregression (QVAR) to model the tail dependence between these prices to determine the likelihood of coinciding high values in the former and low values in the latter price (Joe, 2014). We use a stochastic simulation approach to determine the conditions under which phosphorus recycling becomes profitable. Our study therefore provides three important implications. First, we show if and under which circumstances investments into Phosphorus recovery for dairy processors can become economically viable. Second, we offer a methodological advancement that enables consideration of price dependence in ex-ante investment assessments. Third, we assess the asymptotic stability of the joint price dynamics between phosphorus and energy.

The profitability of phosphorus recycling has been commonly studied with techno-economic analysis, where the input and output quantities of the production process are used to estimate net present values of investments (Daneshgar et al., 2019; Molinos-Senate et al., 2011). Moreover, the costs of recycling are often integrated into environmental life cycle assessments by estimating life cycle costs of one functional unit. However, these analyses often do not consider the profitability of an investment and assume the absence of price risk (cf. Tonini et al., 2019). The phosphorus market has undergone shifts in recent decades, such as the increase of phosphorus production and consumption in China and fertilizer import subsidies in India (Mew et al., 2023). In recent years, the fertilizer market has become more spatially and vertically integrated with the energy market (Bekkerman et al., 2021). Moreover, price volatility is interdependent between agricultural commodities (Gardebroek et al., 2016; Ahmed and Serra, 2015). We extend this literature by modelling the price dependence between phosphorus fertilizer and energy by using QVAR in combination with a copula to simulate the price risk of an investment (Patton, 2013). This approach identifies important implications for both policy makers and investors to support the adoption of recycling technologies and underlying policies that should accelerate this adoption.

Methodologically, we first analyse the structural process of gas, and Diammonium Phosphate (DAP) prices and the food price index (FPI) between 1991–2024 from the World Bank (2024) pink sheet. We model the prices as an autoregressive dynamic process while also considering the tails of the process by conducting Quantile Vector Autoregression (QVAR) (Li and Chavas, 2023). We then use a copula approach in a stochastic simulation of the Net Present Value (NPV) of recycling investments and provide NPV distributions. We thereby identify the likelihood of phosphorus recycling technology becoming profitable and compare our simulation results with standard stochastic simulation approaches that do not consider quantile dependent prices (Spiegel et al. 2021).

We find that phosphorus recycling from dairy processing wastewater is not profitable, and phosphorus and energy price processes do not exhibit a particularly large correlation in the tails. In contrast, correlation between the two price lags occurs around the median of the two commodities. Overall, the price lags of gas and phosphorus are negatively correlated, which leads to a lower variance of the NPV distribution compared to the standard methodology. In addition, we find the price dynamics are less stable when gas prices are high. We find that investment subsidies of about 1.5 million EUR are necessary to make the investment profitable. Savings in disposal costs of around 130 EUR per ton of wastewater sludge could have the same effect. The results stress that phosphorus recycling from dairy processing wastewater is not profitable and policy support is likely necessary for adoption.

The remainder of this paper is structured as follows. In the next section, we stress the importance of investigating the relationship between energy and phosphorus prices in the profitability assessment of phosphorus recycling. We describe the proposition of phosphorus fertilizer recycling and the economic challenges that arise with its implementation. We describe the process of producing recovered fertilizer and the associated inputs and outputs. Next, we position the recent fertilizer price rise in the commodity price volatility debate. We describe how to model the dependence of the price processes for energy and phosphorus markets and their relationship. Furthermore, we consider the asymptotic behaviour of the relationship. Afterwards, we use a Monte Carlo simulation, to assess the profitability of the recycling investment. Subsequently, we present the results of our analysis and close with a critical discussion and conclusion from a policy maker's and investor's perspective.

Phosphorus Recycling

We investigated phosphorus recycling in the context of dairy processing companies. Dairy processors collect raw milk, apply preservation processes, produce, and package products such as milk, cheese, cream and the like. We call these processing firms producers. The producers face two options for dealing with their waste, first their established methods or second by adopting novel recycling technologies. We assume that producers will only adopt the recycling technology if the sum of the expected discounted benefits arising from selling recycled fertilizer or receiving subsidies over the lifespan of the project exceeds the costs of the initial investment and the sum of expected discounted operational costs. That is, if they receive a positive net present value on their investment. We assume that the NPV will determine the adoption (Zilberman et al., 2019). The yearly cash flow R_i of the investment is described by the following equation:

$$R_t = pd_t m_t - pg_t x_t - Z_t \ + \ c_t \tag{1}$$

in which the subscript t denotes a future period. The quantity of recycled phosphorus fertilizer is m_t, its price is pd_t. The natural gas input quantities are denoted by x_t other input expenditures are described by the scalar Z_t. The prices for gas are pg_t. In our later analysis, we consider pg_t and pd_t to follow a joint stochastic distribution. While we acknowledge that there are multiple policy interventions possible, we assume that there will be investment subsidies and regulation on sludge disposal. The most extreme regulation would ban the spreading of processing sludge outright, while more lenient regulation would at least restrict current practices. In any case, we expect that regulation will increase the costs of disposing of dairy processing sludge. The disposal costs of dairy processing waste play a role because increases in the price of disposal, would generate a direct benefit to the dairy processor. The income from saving disposal costs is denoted as c_t. With cash flows we can calculate the NPV of an investment into recycling technology:

$$NPV = \sum_{t=1}^{T} R_t \delta_t - I_0 + S_0 \tag{2}$$

Where $\delta_t = (discount\ rate + 1)^{-t}$ is the discount factor, which is decreasing over time. I_0 is the initial investment in year 0 and S_0 denotes investment subsidies.

Phosphorus recycling aims to produce fertilizer products from waste streams, which have the same functionality as conventional fertilizers (Velasco-Sánchez et al. 2023). Farmers currently use the processing waste as fertilizer in its untransformed sludge form, but this practice faces criticism (Shi et al., 2021). The sludge differs from recycled fertilizers and conventional fertilizer in the following aspects. First, the untreated sludge is not concentrated, thus has a greater mass than recycled fertilizer. Second, sludge also contains volatile compounds, that release odours and are chemically active. The fertilizer components are combined with other reactive waste components in the sludge, making them a potential environmental hazard. Farmers cannot apply the sludge in an effective manner, leading to run off phosphorus pollution (Shi et al., 2021). Thirdly, the sludge composition is very heterogenous over time, making it infeasible to use it for precision fertilization. These reasons make the storage, transportation, and field application of sludge problematic.

Public water utilities have been recycling phosphorus from their waste for years. At the same time private sector firms with wastewater seldomly recycle phosphorus, because unlike public companies they cannot internalize public goods associated with phosphorus recycling (Egle et al., 2014). Societal benefits of both reducing negative externalities and providing public goods arising from phosphorus pollution might justify policy interventions to incentivize the adoption. One way phosphorus recycling reduces negative externalities is by reducing the toxic content of fertilizers compared to processing sludge, another way is by simplifying the export of phosphorus fertilizers to countries reducing country-level nutrient surpluses. In addition, phosphorus recycling creates public goods such as improved water quality and a reduction of trade vulnerabilities (Barbieri et al., 2022).

The recycling of fertilizer entails the chemical and thermal transformation of waste to enhance its characteristics in a favourable way. Technologies to achieve this are similar for a range of different waste types. We focus on Hydrothermal Carbonisation and chemical precipitation technologies as being the most advanced and promising processes (Uhlemann et al., 2024). Hydrothermal carbonization separates dry and wet components in sludge by applying heat and pressure. The application of heat and pressure carbonifies the sludge, which produces a char and a liquid. The char contains fertilizer components and has soil improving properties. Chemical precipitation is then used to extract phosphorus salts from the liquid. The phosphorus salts are similar to rock phosphate-derived fertilizer such as DAP (Shi et al., 2021). Other technologies can be employed to recycle phosphorus, and we describe them in detail in the appendix. All the individual applications have in common, that heat is used to separate undesired components from the fertilizer compounds contained in the waste. This highlights that any form of phosphorus recycling will have at least heat energy as an input and phosphorus fertilizer as an output.

Figure 1 shows the trajectories of the log prices of gas and DAP, we note both price series spikes around the time of the global financial crisis and the Russian invasion of Ukraine. While the fertilizer price spike in 2022 has created a potential for firms to earn profits from selling recycled phosphorus while addressing the phosphorous scarcity problem (Brownlie et al., 2023). As commodity prices are interconnected energy prices have also risen during this time. The fertilizer prices are connected to food and energy markets, as agricultural producers are affected by phosphorus price volatility since fertilizers are an input to agricultural production. Serra and Zilberman (2013) summarize the literature on biofuel related price transmission, concluding that energy prices drive long-run agricultural price levels. Ciaian and d'Artis Kancs (2011) developed a model that explains the relationship between prices of energy and prices of agricultural commodities through an output and an input channel. Among the inputs that determine the price links in their study is fertilizer. Price changes lead to investment risk, that in turn disincentivize the adoption of phosphorus recycling.

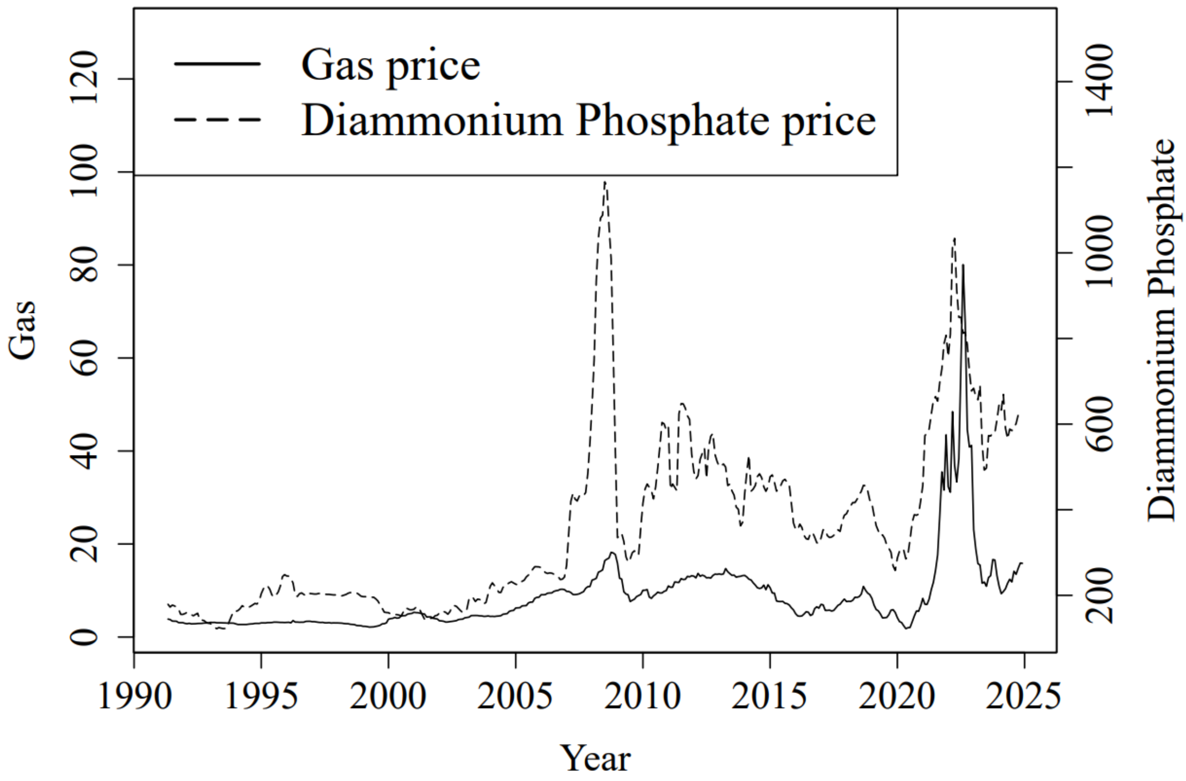

Figure 1: Trajectories of gas price (EUR/GJ) and Diammonium Phosphate price (EUR/mt), 1991–2024

From the above we hypothesize, that the relationship of the individual price movements of energy and phosphorus and their volatility has to be considered when determining the profitability of phosphorus recycling investments in order to correctly reflect the price risks. More specifically, we expect that high phosphorus and low energy prices occurring together is particularly unlikely. The low probability would reduce the window of opportunity for investing into phosphorus recycling.

Empirical Framework

We propose a novel methodology to model the investment profitability by estimating the dynamic price process of DAP and gas, while placing special consideration on the moments of the joint distribution. In the agricultural economic investment literature, stochastic processes have been used to simulate uncertainty in future prices, however mostly relying on the first two moments of price return distribution (Dixit and Pindyck, 1994).

Most prominently, Geometric Brownian Motion processes have been used in investment modelling since they represent well the price movements of financial assets (Dixit and Pindyck, 1994). In contrast, gas and phosphorus prices and their raw commodities are extracted from existing reserves and reserve owners make decisions about extraction based on their expected profit. For higher prices supply the production sector increases output and vice versa. Therefore, such commodity prices have been modelled as mean-reverting processes such as the Ornstein-Uhlenbeck process (Lund, 1991; Spiegel et al. 2021). These two approaches have in common that tail dependencies between different prices are assumed to be zero. Consequently, we compare our combined approach of copula and QVAR modelling and simulation with the standard method using an Ornstein-Uhlenbeck processes.

As this type of phosphorus recycling has not been implemented at scale, there is no revenue data from actual investments for estimation purposes. Thus, simulations are necessary to study the profitability and provide better information for technological research and policy. Sources of risk such as production risk and institutional risk are likely to affect the investment, both sources of risk have not been documented or measured (Uhlemann et al. 2024). The results of this NPV simulation focus on input and output price risk.

We estimate vector autoregressions for each integer quantile of the joint price distribution of gas pg_t and phosphorus pd_t. To include their joint dependence on food prices and shocks therein, we additionally incorporate the food price index (FPI) as pf_t in our analysis (Enders and Holt, 2012). To ease notation, we let $\boldsymbol{p}_t = (pd_t, pg_t, pf_t)$. That is, the prices of the three commodities are formed by the autoregressive dynamic process in (3) where the distribution functions $g(\cdot)$ explain the contemporaneous prices through their lags. This assumes that $g(\cdot)$ is differentiable, and its error e is serially independent with a continuous distribution function.

$$\boldsymbol{p}_t = \begin{bmatrix} pd_t \\ pg_t \\ pf_t \end{bmatrix} = \begin{bmatrix} g_d(\boldsymbol{p}_{t-1}, \dots, \boldsymbol{p}_{t-n}) \\ g_g(\boldsymbol{p}_{t-1}, \dots, \boldsymbol{p}_{t-n}) \\ gf(\boldsymbol{p}_{t-1}, \dots, \boldsymbol{p}_{t-n}) \end{bmatrix} \tag{3}$$

The joint distribution function of the multivariate distribution is described by,

$$F(\boldsymbol{p} \mid \boldsymbol{P}_{t-1}) = Prob(g \quad (\boldsymbol{p}_{t-1}, \dots, \boldsymbol{p}_{t-n} \leq \boldsymbol{p}) \tag{4}$$

where $\boldsymbol{P}_{t-1} = (\boldsymbol{p}_{t-1}, \dots, \boldsymbol{p}_{t-n})$ includes lagged realizations of all prices. Following the approach by Li and Chavas (2023) using Sklar's theorem (Sklar, 1959) we model the multivariate distribution separately by beginning with the marginal distributions (F_d, F_g, F_f) described in (5a-c). The marginal distributions indicate the dependence between prices and their subsequent own price and cross price lags.

$$F_d(pd \mid \boldsymbol{P}_{t-1}) = Prob(g(\boldsymbol{p}_{t-1}, \dots, \boldsymbol{p}_{t-n}) \leq pd) \tag{5a}$$
$$F_g(pg \mid \boldsymbol{P}_{t-1}) = Prob(g(\boldsymbol{p}_{t-1}, \dots, \boldsymbol{p}_{t-n}) \leq pg) \tag{5b}$$
$$F_f(pf \mid \boldsymbol{P}_{t-1}) = Prob(g(\boldsymbol{p}_{t-1}, \dots, \boldsymbol{p}_{t-n}) \leq pf) \tag{5c}$$

The marginal distributions can be used to describe the joint multivariate distribution F with a copula C with the mapping of the marginal distribution (F_d, F_g, F_f), that indicates the contemporaneous dependence between these marginal distributions.

$$F(\boldsymbol{p} \mid \boldsymbol{P}_{t-1}) = C(F_d(pd \mid \boldsymbol{P}_{t-1}), F_g(pg \mid \boldsymbol{P}_{t-1}), F_f(pf \mid \boldsymbol{P}_{t-1})) \tag{6}$$

The analysis proceeds by modelling the marginal distributions (5a-c) with QVAR allowing us to vary price dependencies across quantiles of the distribution including their tails. The joint distribution function is estimated as pair copula-construction (Acar et al., 2012).

Data

Our data set consists of 404 monthly time series of gas prices, DAP prices and the FPI from April 1991 until October 2024. As shown in Table 1, the gas price and the DAP price time series are stationary without transformation, we continue with the stationary first difference of the FPI. All data is taken from the World Bank (2024) Commodity Price Data - The Pink Sheet. As phosphorus price we take the widely traded DAP price from the World Bank database. The price is for the commodity price for free on board in the US Gulf, which was originally gathered by Bloomberg – Green Markets (which was formerly Kennedy Information LLC). While our analysis, focuses on an application in the EU, we assume that the recycled fertiliser is priced with this DAP price as a reference. As the energy price we use the European natural gas price from the same database. Formerly, the gas price was an average of import and spot prices in Europe; since 2015 this measure uses the Netherlands title transfer facility price. The transfer facility price is a gas delivery contract, which is widely used to price gas in the European Union[1]. To control for shocks in the economic environment that affect the relationship between energy and phosphorus price indirectly we also include the food price index (Alam and Gilbert, 2017; Enders and Holt, 2014). The FPI is a differenced quantity weighted indicator of international food prices, the FPI contains all the price information of global food markets. We include it to capture the indirect connection between the price of energy and price of fertilisers through the food price channel (Ciaian and Kancs, 2011; Bekkerman et al. 2021).

[1] Some producers may not purchase gas on these spot markets but hold long term delivery contracts with utility companies. Since the delivery contracts have an insurance effect, the price for gas in these contracts likely is going to be higher and reflect the inherent risk in the commodity price.

Table 1: Summary statistics

Variables	*Gas*	*Diammonium Phosphate*	*Food Price Index*
Min	1.8	122.19	-17.54
Max	80.09	1165.79	15.43
Mean	8.58	358.39	0.15
Standard Deviation	8.61	207.55	2.86
Skew	4.03	1.29	-0.15
Kurtosis	25.35	4.68	10.52
Trend	0.039	1.237	0
KPSS	2.152	3.58	0.043
ADF	-3.69*	-4.21*	-7.77*

*Note: This table presents statistics rounded to the second decimal on monthly gas (EUR/GJ), DAP prices (EUR/mt) and the differenced World Bank FPI, 1991–2024. The trend indicates the monthly change over time. * Denotes the rejection of the null hypothesis at the 5% significance level for the following tests: KPSS is the Kwiatkowski-Phillips-Schmidt-Shin test and ADF is the Augmented Dickey-Fuller test for stationarity.*

Estimation

We estimate the econometric model in equations (3)-(6) using a two-step approach, first estimating the marginal distribution with the QVAR and subsequently the copula. We test the dynamic stability of the dynamic process. Moreover, the estimates are then used to simulate future prices of gas and DAP that can compare to a standard approach of using stochastic processes without co-dependence in net present value simulations.

Estimation of the Marginal Distribution

The marginal distributions are estimated in the form of a Vector Autoregression (VAR) model. We specify a reduced form VAR without trying to identify causal parameters. The VAR allows to estimate lagged own and cross price relations of the marginal distribution. We determine the order n of the parsimonious VAR through common information criteria, such as the Schwarz Bayesian Information Criterion. The VAR based on Ordinary Least Squares (OLS) only allows us to identify conditional mean effects. That is, price dependencies remain constant among all levels of prices, assuming tail correlations to be similar than correlations at average prices. To allow price dependencies to be different across price quantiles, we use Quantile Vector Autoregression (QVAR) to estimate the linear relation between prices for each integer quantile q from 1 to 99 (Koenker, 2005).

$$p_{dq}(q_d \mid \boldsymbol{P}_{t-1}) = \boldsymbol{\beta}_{0,d}(q_d) + \boldsymbol{\beta}_{1,d}(q_d)\boldsymbol{P}_{t-1} \qquad (7a)$$
$$p_{gq}\left(q_g \mid \boldsymbol{P}_{t-1}\right) = \boldsymbol{\beta}_{0,g}(q_g) + \boldsymbol{\beta}_{1,g}(q_g)\boldsymbol{P}_{t-1} \qquad (7b)$$
$$p_{fq}\left(q_f \mid \boldsymbol{P}_{t-1}\right) = \boldsymbol{\beta}_{0,f}(q_f) + \boldsymbol{\beta}_{1,f}(q_f)\boldsymbol{P}_{t-1} \qquad (7c)$$

The $\boldsymbol{\beta}_{0,i}(q_i)$ estimate, where $i \in \{d, g, f\}$ for each of the series, describes the intercept for price $p_i$in quantile q_i. $\boldsymbol{\beta}_{1,d}(q_d)\boldsymbol{P}_{t-1}$ is a matrix of parameters for the conditional effect of each lag and quantile.

The parameters $\hat{\boldsymbol{\beta}}_i$ are estimated with the following optimisation, where ρ_{q_i} is an indicator function relating the conditional function to the quantile by weighting each observation in terms of its distance to the estimated quantile, ensuring that estimates closer to the estimated quantile have the highest weight in the estimation.

$$\hat{\boldsymbol{\beta}}_i(q_i) \in \mathrm{argmin}_\beta \left\{\sum_{t=1}^{T} \rho_{q_i}\left(p_{it} - p_{iq}(q_i \mid \boldsymbol{P}_{t-1},)\right)\right\} \qquad (8)$$

We investigate various functional specifications of the QVAR using the Schwarz Bayesian Information Criterion (SBIC) on the mean regression (VAR)[2]. To conduct inference on the

[2] We supplement the linear model with a time trend and non-linear squared endogenous variables. The Information Criterion indicates that the squared variables slightly improve the parsimony of the model. Nevertheless, we remain with the linear model, as the non-linear specification does not produce a stable price simulation (see Appendix).

estimated parameters, standard errors are constructed by a standard bootstrap procedure. This is advantageous as the autoregressive properties invalidate other more conventional forms of inference (Koenker and Xiao, 2006).

Dynamic Stability

The dynamics of the marginal distribution under study can be characterized in terms of their stability, i.e., the effect of stochastic shocks on the variables (Enders, 2014, Appendix 6.1). The dynamic stability of a system describes the existence of an equilibrium to which the system moves back to after it is stochastically disturbed. The absence of an equilibrium implies that the system reacts unpredictably to perturbations. Thus, in the absence of stability, simulated future price distributions would come with unreasonably large variations. To quantify dynamic stability, we use the characteristic roots of quantile model combinations. We study the roots λ of the autoregressive process of equation (3). More specifically, we evaluate the modulus of the dominant root $|\lambda_d|$; dominant refers to the largest root. The roots can be derived from the Jacobian matrix in (9), which includes partial derivatives of the parameter function.

$$J\Delta\boldsymbol{p}_t = \begin{pmatrix} \frac{\delta pg}{\delta pg_1} & \frac{\delta pg}{\delta pd_1} & \frac{\delta pg}{\delta pf_1} & \frac{\delta pg}{\delta pg_2} & \frac{\delta pg}{\delta pd_2} & \frac{\delta pg}{\delta pf_2} \\ \frac{\delta pd}{\delta pg_1} & \frac{\delta pd}{\delta pd_1} & \frac{\delta pd}{\delta pf_1} & \frac{\delta pd}{\delta pg_2} & \frac{\delta pd}{\delta pd_2} & \frac{\delta pd}{\delta pf_2} \\ \frac{\delta pf}{\delta pd_1} & \frac{\delta pf}{\delta pg_1} & \frac{\delta pf}{\delta pf_1} & \frac{\delta pf}{\delta pg_2} & \frac{\delta pf}{\delta pd_2} & \frac{\delta pf}{\delta pf_2} \\ 1 & 0 & 0 & 0 & 0 & 0 \\ 0 & 1 & 0 & 0 & 0 & 0 \\ 0 & 0 & 1 & 0 & 0 & 0 \end{pmatrix} \qquad (9)$$

In our case, since the marginal distributions are linear, the matrix elements reduce to parameter estimates.

The absolute value of the dominant root $|\lambda_d| < 1$ indicates stability or that the system is converging to the origin. $|\lambda_d| > 1$ indicate instability and divergence to infinity. The special case of $|\lambda_d| = 1$ also indicates stability, but the system converges to an equilibrium rather than the origin or diverges to infinity. Thus, we conduct hypothesis test for $H_0 = |\lambda_d| = 1$ and two alternative hypotheses $H_{a1} = |\lambda_d| < 1$ and $H_{a2} = |\lambda_d| > 1$. For inference we create a distribution of the roots from the bootstrap realization of the QVAR estimation. We generate standard errors by assuming a normal distribution.

Functional Form of the Copula

The estimates for the marginal QVAR from (7a-c) are used to assign quantiles that have the best fit for the estimates over time to generate F_f, F_g and F_d. This is done by calculating $\hat{p}_{iq}(q_i \mid \boldsymbol{P}_{t-1})$ for all t and q, which $\hat{p}_{iq}$ is then compared to the observed p_{it} to find $\hat{q}_{it}$. These quantile distributions are used to estimate the copula connecting the marginal distributions. The copula indicates the contemporaneous co-dependence between the marginal distributions. That is, a function relating the current state of the quantile in l. unconditional copula.

$$C^1(q_1 \mid q_2) = \frac{\partial C_{12}(q_1, q_2)}{\partial dq_2} \Rightarrow \int \ C^1(q_1 \mid q_2)dq = C_{12}(q_1, q\ ) \tag{11}$$

We use the conditional copulas $C^1(q_1 \mid q_2)$ in the simulations further down.

The overall joint distribution function in F in equation (6) takes the form of the FPI F_f and the two copulas $C_d(F_d \mid F_f)$ and $C_g(F_g \mid F_f)$, in which the DAP price is conditional on the FPI the gas price is conditional on the FPI, respectively. The copulas are also estimated with quantile regression on the inverse quantile of the marginal distribution. The copulas C_d and C_g are estimated with conditional distribution functions D_d and D_g that take the following form:

$$D_d(q_d \mid q_f) = \boldsymbol{\gamma}_{\boldsymbol{d},\mathbf{0}}(q_d) + \boldsymbol{\gamma}_{\boldsymbol{d},\mathbf{1}}(q_d)q_f \tag{12a}$$
$$D_g(q_g \mid q_f) = \boldsymbol{\gamma}_{\boldsymbol{g},\mathbf{0}}(q_g) + \boldsymbol{\gamma}_{\boldsymbol{g},\mathbf{1}}(q_g)q_f \tag{12b}$$

Simulation

The estimates of the two proceeding steps are the foundation for the simulation of price series from the joint distribution. The following algorithm is used to create a distribution over P simulation paths and the investment horizon T. We choose the planning horizon of 15 years corresponding to 180 months, a common planning horizon for engineering problems. This rather long planning horizon highlights the problem of stability, as unstable dynamics tend towards infinite prices over time. We simulate q_1^*, q_2^* and q_3^* with a uniform distribution for each integer quantile (1-99) (Wang et al., 2024).

1. The first random number q_1^* selects the quantile of the FPI marginal to predict the current observation based on the past observations.

$$\beta_f(q_1^*) * \boldsymbol{P}_{t-1} = pf_t \tag{13a}$$

2. q_1^* also selects the quantiles of the two copulas distribution $\boldsymbol{\gamma_d}$ and $\boldsymbol{\gamma_g}$, which are fitted with the respective random draws q_2^* and q_3^*. The fitted $\hat{q}_4$ and $\hat{q}_5$ reflecting contemporaneous dependence through the two bivariate copulas distributions.

$$q_2^* * \boldsymbol{\gamma_d}(q_1^*) = \hat{q}_4 \tag{13b}$$

$$q_3^* * \boldsymbol{\gamma_g}(q_1^*) = \hat{q}_5 \tag{13c}$$

3. $\hat{q}_4$ and $\hat{q}_5$ select the quantiles for the DAP and the gas price marginals. The selected quantile estimates with past observation predict the current DAP and the gas price.

$$\boldsymbol{\beta_d}(\hat{q}_4) * \boldsymbol{P}_{t-1} = pd_t \tag{13d}$$

$$\boldsymbol{\beta_g}(\hat{q}_5) * \boldsymbol{P}_{t-1} = pg_t \tag{13e}$$

The simulation draws are then used to calculate NPVs based on equations (1) and (2), as well as additional parameters describing the phosphorus recycling investments that are described in the appendix.

Stochastic Processes

The QVAR methodology allows us to estimate the shapes of the conditional distribution. We compare the QVAR simulations to simulations with Ornstein-Uhlenbeck processes, which only incorporate a mean and a diffusion parameter in the simulation and do not incorporate dependence between prices. The price change in a month δp is indicated by,

$$\delta pg_t = \mu_g(\theta_g - pg_t)\delta t + \sigma_g \delta W_t^g \tag{14a}$$

$$\delta pd_t = \mu_d(\theta_d - pd_t)\delta t + \sigma_d \delta W_t^d \tag{14b}$$

Where θ indicates the long run mean, μ is a parameter that indicates the speed of the mean reversion, σ indicates the dispersion of the Wiener process δW_t . These parameters are estimated from the same price observation, the estimation procedure is explained in the appendix.

Environmental Policies

Policy makers place attention on phosphorus recycling because it provides a multitude of positive externalities like pollution reduction, waste disposal and phosphorus supply security as detailed in the introduction. These positive externalities generally lead to a gap between private investment incentives and optimal investment levels. As a result of this, we deem it worthwhile to include potential political interventions and their impact on the NPV distribution in the analysis. In addition, we will consider the firm perspective on the investment decision under the higher moments of price volatility.

First, we quantify the required investment subsidy to shift all simulated scenarios so that they have a positive NPV. Second, we quantify the required investment subsidy so that the average NPV is equal to zero. A major argument for phosphorus recycling is waste disposal (Uhlemann et al. 2024). Thus, we quantify the two measures in terms of the monetary benefit, the investing firm would need to gain from recycling phosphorus from a ton of waste sludge. Third, we focus on the certainty equivalent CE of the investment. The certainty equivalent is certain payment, which provides the decision maker with the equivalent utility as the uncertain investment decision. The CE is the expectation of the NPV π subtracted by the risk premium RP.

$$CE = E(\pi) - RP \tag{15}$$

The risk premium is a function of investor's level of risk aversion and the second and the third moment of the profit distribution. Following Conradt et al. (2015) we use a negative exponential utility function,

$$U = 1 - e^{-r_a * \pi} \tag{16}$$

where r_a is the risk aversion parameter and π represents the firms net present value. The risk premium can be approximated by the Taylor expansion $RP \approx \sum_{i=2}^{k} -\frac{1}{i!}\frac{U^i}{U^1}M^i$, where $M^i = E[\pi - E(\pi)]^i$ and $U^i = \frac{\partial^i U}{\partial \pi}$. Thus, the risk premium for the negative exponential function is

$$RP \approx 1/2 * r_a * \sigma_\pi^2 - 1/6 * r_a^2 * \sigma_\pi^3. \tag{17}$$

Results

In this section we first show the conditional Quantile Vector Autoregression (QVAR) distributions of the gas prices, DAP prices and FPI, respectively. Second, we present the outcomes of the copula model which provides a valid joint distribution of the dependence between the two prices. Here, we observe a relation between the two prices, this relationship is not skewed in a particular direction. Third, we estimate the quantile stability of the dynamic process. Fourth, we compare the QVAR price simulation results to the simulation of the Ornstein-Uhlenbeck processes. Finally, we use NPV distributions to determine the profitability of the phosphorus recycling investment.

QVAR

The results of the QVAR model (see appendix table A2-A4) show that the gas price is mostly correlated to its own lags, while the DAP price is also correlated to the lags of other variables. All correlations are stronger around median prices and weaker in the tails of the price distributions. For the marginal distribution, the Schwarz Bayesian Information Criterion (SBIC) indicates that a VAR of order two is parsimonious. We compare this with several different specifications (The specifications and their information criteria are described in Appendix C). While the SBIC improves when we add non-linear terms, but not with a linear trend. We further consider specification (1) and (4). The following description corresponds to specification (1)[3]. Bootstrap standard errors are used to conduct hypothesis tests on the QVAR estimates. Appendix C additionally includes Figure A1 and A2 showing the probability density functions of the observed and the simulated prices.

[3] The results correspond to this equation $\boldsymbol{P}_{t-1} = pg_{t-1} + pd_{t-1} + pf_{t-1} + pg_{t-2} + pd_{t-2} + pf_{t-2}$. The other specifications include (2) additional third lag, (3) a linear time trend, (4) squared first lag for the gas and DAP prices and (5) a linear time trend as well as squared first lag for the gas and DAP prices.

We find the lagged own price effects are most often significant. The gas price is significantly affected by all its own lags. In the OLS VAR regression, the first lag coefficient of (standard error: 0.049) means that an increases of the gas price of one EUR in the previous month is significantly correlated with a contemporaneous price increase of 1.076 EUR. Conversely, increases in the second lag of the gas price decrease the contemporaneous price. The FPI correlation with the gas price is only significant in the second lag, while the effect of DAP is significant on the first lag. The R^2 of the VAR on the gas price is 0.91. There is considerable fluctuation of the Pseudo-R^2 of the quantile regressions, the Pseudo-R^2 of the lower tails of the gas price is lower indicating that the explanatory power of the model decreases for lower prices. The DAP price is positively and is significantly affected by the first, and negatively by the second lag of its own price. The FPI effect on the DAP price is significant in the higher quantiles of the first lag. The VAR R^2 is very high at 0.98, showing that a large fraction of the variation in the DAP price can be explained by the lags in the model. The own price effect of the FPI is significant and positive in the first lag. The second lag is only significant in the 90th quantile. The other correlations are not significant. The VAR R^2 is 0.19 showing less of the variation of the FPI is explained in the model. The Pseudo-R^2 indicate that the model explains more variation in the upper and lower tails of the FPI. The These results for all three dependent variables vary across quantiles, the effects remain strongest in the median regressions, dissipating in the tails.

Copula

We use the results of the QVAR models to estimate the two quantile copula from equation (12 a-b) of the marginal distributions using bootstrapping to estimate the standard errors. The results can be found in the appendix tables A5 and A6. The regression results indicate how the marginal distributions are correlated contemporaneously. The linear correlation between the FPI and the gas price distribution is only significant in the 10th quantile indicating co-movement when gas prices are low. Here, the FPI distribution positively affects increases in the DAP price in the 70th quantile. The constants in both regression specification and across quantiles are mostly positive and significant. The coefficients increase across quantiles, leading the constant coefficients to roughly correspond to their quantiles regardless of the independent variable. None of the parameters are negative, indicating that the prices do not move in opposite directions.

Stability

Table 2 shows the modulus of the dominant root $|\lambda_d|$ for different quantiles of phosphorus and gas prices under median FPI. The results show that the dynamic instability is prevalent amongst the higher gas price quantiles 0.7 and 0.9. The DAP price quantiles are stable for lower gas prices and unstable for higher gas prices. The tables A7 and A8 in the Appendix report these results for the 0.1 and 0.9 quantiles of the FPI. While the dynamic stability at the 0.1 quantile of the FPI is fairly similar to the median results, the 0.9 quantile increases the frequency of dynamic stability. All $|\lambda_d|$ in the 0.9 quantile of the FPI and DAP indicate instability. Overall, the results indicate that the gas price is the most important determinant for dynamic instability, additionally dynamic instability generally occurs in the higher quantiles. From that we can conclude, prices diverge more when prices are high.

Table 2: Modulus of the dominant root for selected has and DAP quantiles at the median FPI

q_d / q_g	0.1	0.3	0.5	0.7	0.9
0.1	0.819 (0.00181)	0.929 (0.00115)	0.976 (0.00067)	1.004 (0.00075)	1.045 (0.00116)
0.3	0.884 (0.0015)	0.937 (0.00083)	0.978 (0.00055)	1.007 (0.00061)	1.051 (0.00091)
0.5	0.957 (0.00131)	0.969 (0.00085)	0.987 (0.00053)	1.013 (0.00052)	1.052 (0.00082)
0.7	1.018 (0.0025)	1.024 (0.00234)	1.031 (0.0022)	1.052 (0.0019)	1.086 (0.00156)
0.9	1.305 (0.00517)	1.306 (0.00513)	1.307 (0.00508)	1.31 (0.00491)	1.316 (0.00467)

Note: The table shows the estimated modulus from the dominant root $|\lambda_d|$. The bootstrap standard errors are below in parenthesis. q_d indicates the DAP quantile, q_g indicates the gas quantile.

Simulation

We use the QVAR estimates to simulate the multivariate distribution of the gas and the fertilizer prices. The simulation for specification (4) produces unrealistic price scenarios that go to infinity; thus, we will present the simulation results for specification (1). The price simulations are then used to calculate the distribution of net present values (NPVs). Finally, we compare the results with simulations from the Ornstein-Uhlenbeck processes (OUP). The parameters for the simulation are found in Table 3.

Table 3: Parameters for the stochastic processes

	Gas price	Diammonium Phosphate Price
Long-run mean θ	8.93	393.41
Speed of reversion μ	0.05	0.015
Standard deviation σ	1.99	24.02

Note: this table indicates the parameters used in simulating the Ornstein-Uhlenbeck processes

Our analysis shows that all simulated NPVs are negative. The QVAR NPV distribution has thinner tails and higher kurtosis than the OUP NPV distribution. This result reflects the negative correlation between the lags in the QVAR being more important than the positive correlation of the copulas between the FPI and the gas price distribution and the FPI and the DAP price distribution. Consequently, the QVAR NPV distribution exhibits second-order stochastic dominance over the OUP NPV distribution.

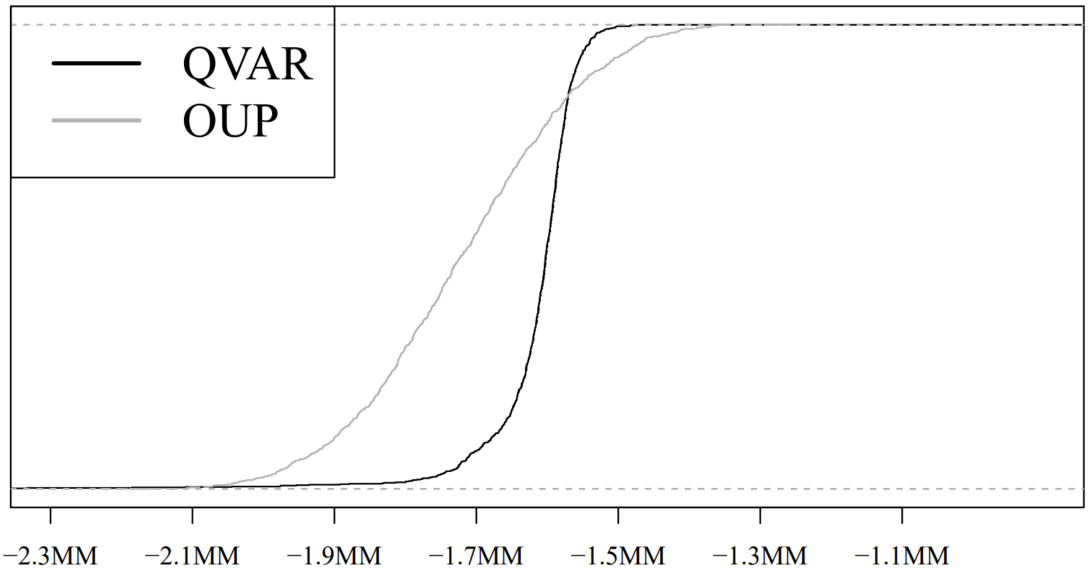

Figure 2a: Cumulative density of NPV of investments into phosphorus recycling from dairy wastewater. Simulations based on quantile vector autoregression (QVAR) and Ornstein-Uhlenbeck Processes (OUP) representation of underlying price processes.

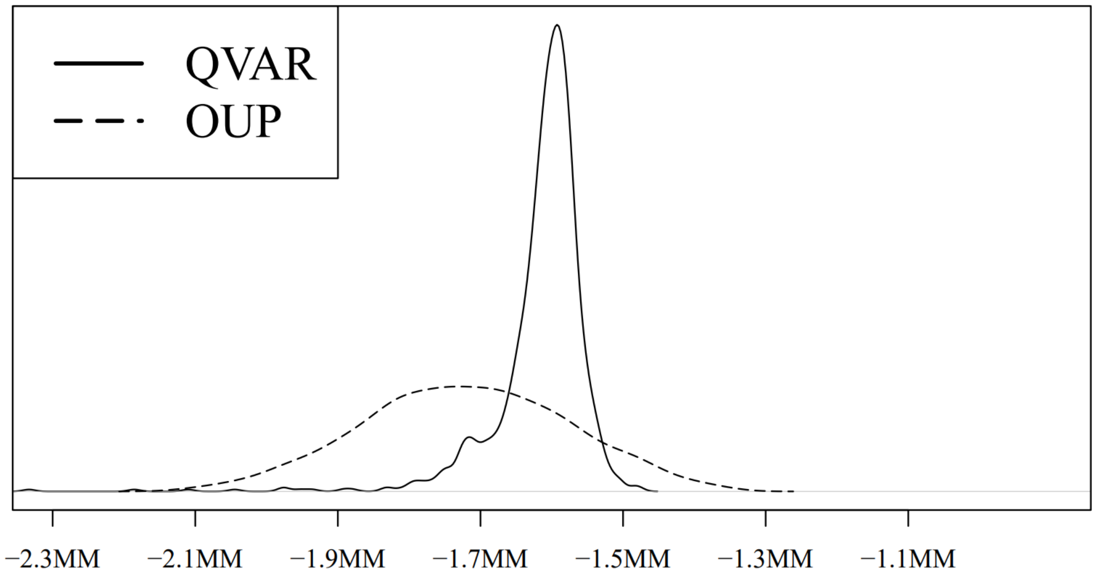

Figure 2b: Kernel density of NPV of investments into phosphorus recycling from dairy wastewater. Simulations based on quantile vector autoregression (QVAR) and Ornstein-Uhlenbeck Processes (OUP) representation of underlying price processes.

The summary statistics in Table 4 show that the flexible QVAR simulations result in an NPV distribution that has a mean of about -1.6 million EUR while the OUP simulation's mean is lower at -1.7 million EUR. The standard deviation of the distribution at 74,605 is about half of the OUP's at 142,089. We conduct statistical tests for skewness and kurtosis. There, we find that the QVAR distribution has significant skew of -5.55, while the OUP skewness is not significantly different from zero. The Anscombe test finds that the QVAR distribution is leptokurtic indicating flat tails, while the OUP distribution is platykurtic or heavy-tailed.

Table 4: Summary statistics of the NPV simulations

Variables	*QVAR*	*OUP*
Min	-2,689,252	-2,093,424
Max	-1,477,048	-1,352,070
Mean	-1,616,032	-1,709,716
Standard Deviation	74,605	142,089.4
Skew	-5.55***	-0.03
Kurtosis	61.05***	2.67***

Note: The ***, ** and * in the skew and kurtosis rows indicate the rejection of the null hypothesis at the 1,5, and 10 % percent level with the respective Agostino and Anscombe test indicating the absence of skew or kurtosis.

Environmental Policies

Phosphorus recycling is the focus of political considerations, which could have considerable effects on the revenue of phosphorus recycling. The results in Table 5 show that the calculated investment subsidy and the required disposal costs are not sensitive to the different investment thresholds. The break-even revenue from avoiding sludge disposal is lower than the potential costs for sludge disposal of 250 EUR described in Medina-Martos et al. (2020). For the mean NPV threshold we see that disposal costs of around 130 EUR would make recycling profitable, this corresponds to a 37 % subsidy of the mean DAP price[4].

[4] 133.92 / 358.39 ≈ 0.37

Table 5: Necessary policy interventions to reach policy targets.

Interventions	Policy targets	
	(1) All positive profit	(2) Average profit of zero
Investment subsidy in EUR	2,689,252	1,616,032
Avoiding the disposal of sludge in EUR/mt	222.86	133.92

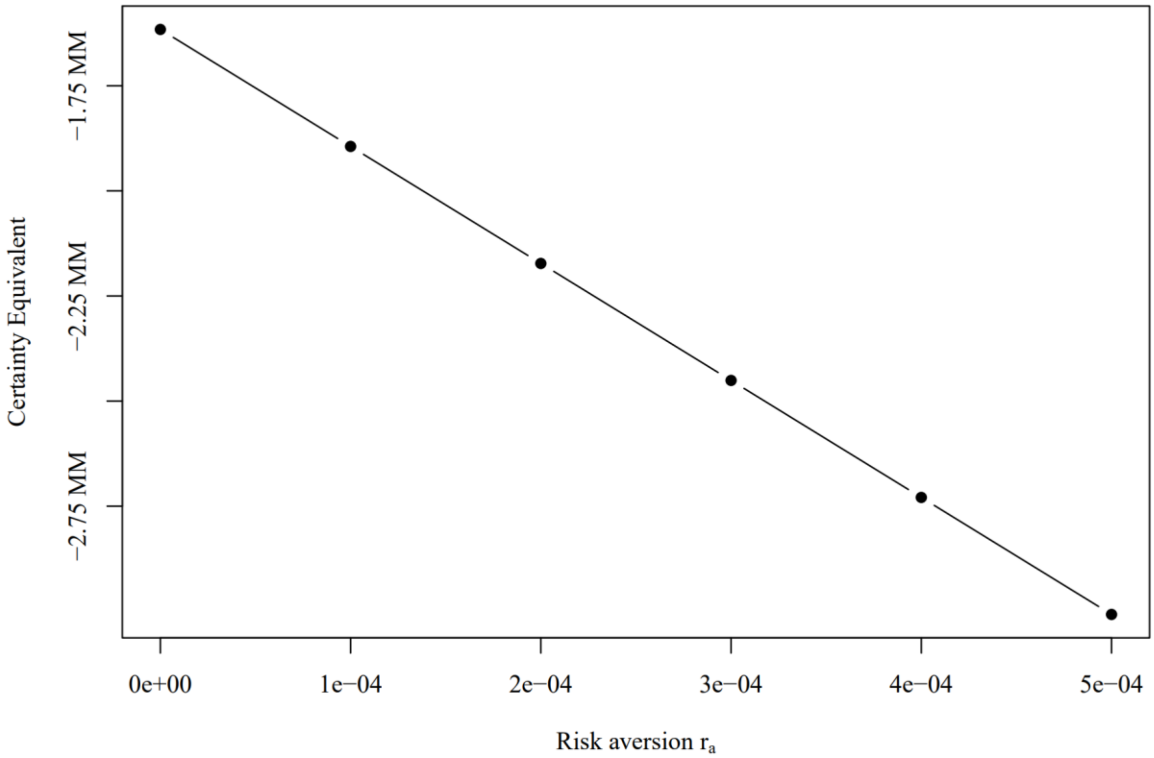

Figure 3: Function of certainty equivalents with respect to risk aversion in EUR.

The certainty equivalents in Figure 4 imply that even at a negligible risk aversion level of 0,0003 the mean NPV doubles due to the high variance of the NPV distribution. The skewness of the of the NPV distribution only contributes minimally to the certainty equivalent leading to a linear function. Since the certainty equivalent is negative, we can interpret the values in figure

4 as minimum required subsidies in order to make decision makers with the respective x-axis risk aversion level choose to invest in phosphorus recycling with uncertain profitability. Thus, if policy makers want firms to invest in phosphorus recycling, they would have to compensate the firms in with the certainty equivalent. The results indicate that even at low risk aversion levels firms might require subsidies that are much higher than the mean NPV.

Discussion

Quantile Vector Autoregression (QVAR) combined with two bivariate copulas allowed us to investigate the structure of the multivariate distribution of the prices of food, gas, and Diammonium Phosphate (DAP). We find that the negative correlation between the gas and the DAP price lags, particularly around the median, combined with low tail dependence, results in lower variance of the NPV distribution compared to standard investment assessments that do not consider price dependence. These results differ from other results looking at market integration of nitrogen fertilizer and energy markets in the United States (Bekkerman et al., 2021). This difference might stem from energy being even more crucial in nitrogen fertilizer production than in phosphorus recycling. Moreover, price dynamics are less stable when gas prices are high. Although our newly established methodology results in a lower variance of the NPV distribution from investing in phosphorus recycling, the entire distribution is negative. While findings from Uhlemann et al. (2024) suggest that phosphorus recycling can become profitable with a combination of high phosphorus and low energy prices, our results show that this scenario is highly unlikely. In addition, our work provides methodological innovations, such as flexibly modelling price time series and employing the estimates to simulate NPVs, that should be considered in future investment studies where prices are dependent on each other.

We modelled the future price of recycled phosphorus fertilizers by assuming that they are close substitutes for conventional fertilizer and will therefore have the same price. However, on a critical note, recycled fertilizers still must prove whether they can substitute for conventional fertilizers in terms of fertilizing effectiveness (Velasco-Sánchez et al. 2023). Policies could introduce standards that ensure agronomic equivalence of recycled fertilizers. In addition to the political interventions, we quantified (investment subsidies and savings through avoiding sludge disposal), policymakers might also incentivize the adoption of phosphorus recycling by increasing the relative price of recycled fertilizer compared to conventional fertilizers, which could make investments profitable (Koppelar and Weikard, 2013). Our empirical framework can be extended to assess such policy interventions.

We now proceed to discuss limitations that stem from assumptions that were necessary to conduct the research. Our method of estimating investment risk only captures price risk. Future research might complement this by also considering other sources of risk. An analysis of production risk can identify common shocks that change the production function of phosphorus recycling (Lien et al., 2022). Potential shocks could be the breakdown of machinery or heterogeneity in sludge. The analysis of policy risks can investigate the manner, the likelihood, and magnitude of potential regulation on phosphorus recycling (Dixit and Pindyck, 1994). Policies on the other hand might also play a significant role in the handful of phosphorus producing countries. While often state-owned phosphorus mining companies might have incentives to provide domestic farmers with affordable fertilizer, other companies might focus purely on profit maximization from phosphorus mining. Therefore, idiosyncratic shocks in specific phosphorus-producing countries might affect phosphorus policies (e.g., on trade) in these countries which can have heterogeneous effects on global phosphorus markets. To provide a more nuanced reflection of these potentially heterogenous effects across producing countries, future research might engage in estimating producer specific supply curves and simulating country specific shock and policy scenarios which in turn could further improve the reflection of risk in phosphorus price related investments (Mew et al., 2023).

The negative NPV distribution with a large standard deviation indicates that the price risk results in significant investment risk and non-profitability. Our here proposed procedure can be considered as a first step of a more extensive investment assessment. However, due to the negative returns and high risk of the investment, it is unlikely that investors will pursue such a project without further technological developments and or investment support. Yet, future research could more explicitly consider future technological development that makes the recycling process more efficient and thereby more profitable. Furthermore, policy instruments and their likelihood of being implemented can also be a useful extension of our model in future research. If such technological changes materialize and supporting policies are implemented, investments in phosphorus recycling might become less risky and more profitable. In case this is fulfilled, further research could use Real Options Theory to better model investors' behaviour in a positive modelling setting or derive optimal decision making in a normative way towards such an analysis. Regarding the further policy support, beyond subsidies and saved disposal cost considered here, other policies such as tradable pollution permits, a tax on unrecycled phosphorus or requirements for recycled fertilizer in commercial fertilizers could raise the incentives of the investment and be an interesting entry point for future research. Moreover, future research should attempt to validate our results in a real-world setting using observational data as soon as investments into phosphorus recycling are realized. Especially, the potential disposal savings could be investigated in regions where the application of dairy processing sludge as a fertilizer is already restricted.

Phosphorus is exchanged between countries through trade of phosphorus minerals and agricultural commodities, which are produced with phosphorus and subsequently exported. Barbieri et al. (2021) call this telecoupling and document the resulting threats to food system resilience due to the dependence of many importers on few exporters. The phosphorus in the soil has become scarce due to agricultural practices, while food production waste is rich in phosphorus. This creates a paradox of simultaneous phosphorus scarcity and abundance. To address this, phosphorus recycling is highlighted as a way to reduce both phosphorus scarcity and pollution, thereby creating a more resilient food system. Brownlie et al. (2021) posit the concept of phosphorus vulnerability analysing the potential impacts of shocks of the phosphorus system along the dimensions of exposure to shocks, the sensitivity to said shocks, and potential adaption pathways. Again, here widespread phosphorus recycling is seen as a crucial lever to achieve sustainable food systems. However, our analysis shows that without substantial public support, the adoption of recycling technologies is highly unlikely.

Conclusion

Phosphorus recycling is regarded as a key strategy for closing phosphorus cycles and reducing dependence on phosphorus imports. We found that the dynamic processes of phosphorus and gas prices are correlated. Moreover, this dynamic process remains stable in the lower part of the distribution, but high gas prices significantly increase instability. Our results indicate that phosphorus recycling entails substantial economic costs for investors. In fact, investments in phosphorus recycling from dairy processing wastewater are unprofitable in all simulation iterations. Unlike earlier studies with ambiguous findings on recovery profitability, our results clearly indicate that phosphorus recycling from dairy wastewater is not viable without significant policy support, making private investment highly unlikely.

Our results have implications for various stakeholders of phosphorus recycling namely policy makers, the food industry, and future research. Based on our results, policymakers should not expect phosphorus recycling to simultaneously solve sustainability issues and remain profitable for recyclers. Achieving sustainable waste disposal with current technologies requires substantial policy interventions. The food sector should integrate financial decision-making about waste recycling into its risk management, potentially enabling a more optimal investment portfolio than the single-decision approach considered here. Moreover, our results reveal a gap between the aspirations for phosphorus recycling and its current feasibility. Research on recycling should also examine how businesses decide in favour of recycling, beyond just technological innovation. In addition to the economic hurdles, environmental considerations of the large energy demand of the recycling process present further challenges (Behjat et al., 2022). Methodologically, we provide an approach to more precisely quantify investment risk in settings with non-linear input- and output-price price dependence of the investment.

In conclusion, we provide evidence on the quantile correlation between phosphorus and gas prices to assess the investment risk of novel phosphorus recycling applications. This approach enables us to simulate the price risk within historical multivariate price distribution, offering insights into the feasibility of new technology investments. Currently, phosphorus recycling from dairy processing wastewater is not profitable, exacerbated by variation in the net present value due to price risk. To increase the adoption of phosphorus recycling, the investments should be supported by targeted policies such as investment subsidies, waste disposal payments and compensation for positive externalities.

References

Acar, E. F., Genest, C., and Nešlehová, J. (2012). Beyond simplified pair-copula constructions. *Journal of Multivariate Analysis 110*: 74–90.

Ahmed, O., and Serra, T. (2015). Economic analysis of the introduction of agricultural revenue insurance contracts in Spain using statistical copulas. *Agricultural Economics 46*: 69–79.

Alam, M. R., and Gilbert, S. (2017). Monetary policy shocks and the dynamics of agricultural commodity prices: evidence from structural and factor-augmented VAR analyses. *Agricultural Economics 48*: 15–27.

Barbieri, P., MacDonald, G. K., Bernard de Raymond, A., and Nesme, T. (2022). Food system resilience to phosphorus shortages on a telecoupled planet. *Nature Sustainability 5*: 114–122.

Bekkerman, A., Gumbley, T., and Brester, G. W. (2021). The Impacts of Biofuel Policies on Spatial and Vertical Price Relationships in the US Fertilizer Industry. *Applied Economic Perspectives and Policy 43*: 802–822.

Brownlie, W. J., Sutton, M. A., Cordell, D., Reay, D. S., Heal, K. V., Withers, P. J. A., Vanderbeck, I., and Spears, B. M. (2023). Phosphorus price spikes: A wake-up call for phosphorus resilience. *Frontiers in Sustainable Food Systems 7*.

Brownlie, W. J., Sutton, M. A., Reay, D. S., Heal, K. V., Hermann, L., Kabbe, C., and Spears, B. M. (2021). Global actions for a sustainable phosphorus future. *Nature Food 2*: 71–74.

Ciaian, P., and Kancs, D. (2011). Food, energy and environment: Is bioenergy the missing link? *Food Policy 36*: 571–580. Scopus.

Conradt, S., Finger, R., and Bokusheva, R. (2015). Tailored to the extremes: Quantile regression for index-based insurance contract design. *Agricultural Economics 46*: 537–547.

Daneshgar, S., Buttafava, A., Callegari, A., and Capodaglio, A. G. (2019). Economic and energetic assessment of different phosphorus recovery options from aerobic sludge. *Journal of Cleaner Production 223*: 729–738.

Dixit, A. K., and Pindyck, R. S. (1994). *Investment under uncertainty* , 2523944. Princeton, N.J.: Princeton University Press.

Egle, L., Rechberger, H., Krampe, J., and Zessner, M. (2016). Phosphorus recovery from municipal wastewater: An integrated comparative technological, environmental and economic assessment of P recovery technologies. *Science of The Total Environment 571*: 522–542.

Enders, W. (2014). *Applied Econometric Time Series*. Hoboken, NJ.:

Enders, W., and Holt, M. T. (2014). The evolving relationships between agricultural and energy commodity prices: a shifting-mean vector autoregressive analysis. In *The Economics of Food Price Volatility*. University of Chicago Press , 135–187.

European Commission. (2020). *A new Circular Economy Action Plan For a cleaner and more competitive Europe* [COMMUNICATION FROM THE COMMISSION]. https://eur-lex.europa.eu/legal-content/EN/TXT/?uri=COM:2020:98:FIN , last accessed

Finger, R. (2013). Expanding risk consideration in integrated models – The role of downside risk aversion in irrigation decisions. *Environmental Modelling & Software 43*: 169–172.

Gardebroek, C., Hernandez, M. A., and Robles, M. (2016). Market interdependence and volatility transmission among major crops. *Agricultural Economics 47*: 141–155.

Joe, H. (2014). *Dependence Modeling with Copulas*. New York: Chapman and Hall/CRC.

Khalaf, N., Shi, W., Fenton, O., Kwapinski, W., and Leahy, J. (2022). Hydrothermal carbonization (HTC) of dairy waste: effect of temperature and initial acidity on the composition and quality of solid and liquid products [version 2; peer review: 1 approved with reservations]. *Open Research Europe 2*.

Koenker, R. (2005). *Quantile Regression*. Cambridge: Cambridge University Press.

Koenker, R., and Machado, J. A. F. (1999). Goodness of Fit and Related Inference Processes for Quantile Regression. *Journal of the American Statistical Association 94*: 1296–1310.

Koenker, R., and Xiao, Z. (2006). Quantile Autoregression. *Journal of the American Statistical Association 101*: 980–990.

Li, J., and Chavas, J.-P. (2023). A dynamic analysis of the distribution of commodity futures and spot prices. *American Journal of Agricultural Economics 105*: 122–143.

Lien, G., Kumbhakar, S. C., Mishra, A. K., and Hardaker, J. B. (2022). Does risk management affect productivity of organic rice farmers in India? Evidence from a semiparametric production model. *European Journal of Operational Research 303*: 1392–1402.

Lund, D. (1993). The Lognormal Diffusion Is Hardly an Equilibrium Price Process for Exhaustible Resources. *Journal of Environmental Economics and Management 25*: 235–241.

Medina-Martos, E., Istrate, I.-R., Villamil, J. A., Gálvez-Martos, J.-L., Dufour, J., and Mohedano, Á. F. (2020). Techno-economic and life cycle assessment of an integrated hydrothermal carbonization system for sewage sludge. *Journal of Cleaner Production 277*: 122930.

Mew, M., Steiner, G., Haneklaus, N., and Geissler, B. (2023). Phosphate price peaks and negotiations – Part 2: The 2008 peak and implications for the future. *Resources Policy 83*: 103588.

Molinos-Senante, M., Hernandez-Sancho, F., Sala-Garrido, R., and Garrido-Baserba, M. (2011). Economic Feasibility Study for Phosphorus Recovery Processes. *Ambio 40*: 408–416.

Patton, A. (2013). Copula Methods for Forecasting Multivariate Time Series. In *Handbook of Economic Forecasting* (Vol. 2). Elsevier , 899–960.

Richardson, K., Steffen, W., Lucht, W., Bendtsen, J., Cornell, S. E., Donges, J. F., Drüke, M., Fetzer, I., Bala, G., von Bloh, W., Feulner, G., Fiedler, S., Gerten, D., Gleeson, T., Hofmann, M., Huiskamp, W., Kummu, M., Mohan, C., Nogués-Bravo, D., … Rockström, J. (2023). Earth beyond six of nine planetary boundaries. *Science Advances 9*: eadh2458.

Serra, T., and Zilberman, D. (2013). Biofuel-related price transmission literature: A review. *Energy Economics 37*: 141–151.

Shi, W., Healy, M. G., Ashekuzzaman, S. M., Daly, K., Leahy, J. J., and Fenton, O. (2021). Dairy processing sludge and co-products: A review of present and future re-use pathways in agriculture. *Journal of Cleaner Production 314*: 128035.

Sklar, M. (n.d.). *Fonctions de répartition à N dimensions et leurs marges*.

Spiegel, A., Britz, W., and Finger, R. (2021). Risk, Risk Aversion, and Agricultural Technology Adoption — A Novel Valuation Method Based on Real Options and Inverse Stochastic Dominance. *Q Open 1*: qoab016.

Springmann, M., Clark, M., Mason-D'Croz, D., Wiebe, K., Bodirsky, B. L., Lassaletta, L., de Vries, W., Vermeulen, S. J., Herrero, M., Carlson, K. M., Jonell, M., Troell, M., DeClerck, F., Gordon, L. J., Zurayk, R., Scarborough, P., Rayner, M., Loken, B., Fanzo, J., … Willett, W. (2018). Options for keeping the food system within environmental limits. *Nature 562*: 519–525.

Tonini, D., Saveyn, H. G. M., and Huygens, D. (2019). Environmental and health co-benefits for advanced phosphorus recovery. *Nature Sustainability 2*: 1051–1061.

Uhlemann, J.-P. R., Oude Lansink, A., Leahy, J. J., and Dalhaus, T. (2024). Do investments in phosphorus recovery from dairy processing wastewater pay off? *Journal of Environmental Management 357*: 120606.

Velasco-Sánchez, Á., Bennegadi-Laurent, N., Trinsoutrot-Gattin, I., van Groenigen, J. W., and Moinet, G. Y. K. (n.d.). Soil microorganisms increase Olsen phosphorus from poorly soluble organic phosphate: A soil incubation study. *Soil Use and Management n/a*.

Wang, L., Chavas, J., and Li, J. (2024). Dynamic linkages in agricultural and energy markets: A quantile impulse response approach. *Agricultural Economics 55*: 639–676.

World Bank. (2024). *CMO Pink Sheet May 2024*. https://thedocs.worldbank.org/en/doc/5d903e848db1d1b83e0ec8f744e55570-0350012021/related/CMO-Pink-Sheet-November-2023.pdf , last accessed

Zilberman, D., Lu, L., and Reardon, T. (2019). Innovation-induced food supply chain design. *Food Policy 83*: 289–297.

Appendix A: Phosphorus Recycling

Potential Pathways

For a better understanding of the research subject, we describe possible recycling pathways. The recycling process can consist of a single application or a combination of different steps, namely drying, Hydrothermal Carbonization, Pyrolysis, Precipitation, and Incineration. Drying is usually the first step in treating wastewater sludge, the drying can vary in its energy intensity by the degree of technology and time as an input. The drying step mitigates runoff and storage issue but does not address the fertilizing effect and potential toxicity of waste sludge. Pyrolysis is similar to Hydrothermal Carbonization with higher pressure and higher temperature. During Incineration, the organic components of the sludge are burned, which yields an ash that can easily divided in its components (Kabbe and Rinck-Pfeiffer 2019).

Model Parameters

The values for the estimation are taken from Uhlemann et al. (2024). We choose the technically efficient process specification from Khalaf et al. (2022) for the NPV calculation. The parameters describe the monthly cashflow of the investment model.

83333.383 kg of sludge = 100,000 t of milk /12 months * 10 kg /t of sludge per milk

83333.33 kg of sludge * 73.04% recovery ratio * 0.05717706 phosphorus per kg of sludge

Exchange rate: 1 EUR to 1.08 Dollar

- I: Investment cost for Hydrothermal Carbonization and Precipitation in EUR
    - 1,038 T EUR = 252 T EUR + 786 T EUR
- x: Gas usage in EUR/megajoule
    - 0.9883244 kWh per kg of sludge = 3557.968 KJ

    - 296.4973 GJ = 296497308.36 kJ = 3557.968 KJ per kg of sludge * 83333.33 kg
- Z: Additional production costs in: EUR
    - 4285.687 = 0.05142825 EUR per kg of sludge * 83333.33 kg
- Disposal Savings:
    - 83333.33 kg / 1000kg/t * 245 EUR/T = 20416.67 EUR
- q: DAP price in EUR/metric tons
- Phosphorus content in DAP: 46 %
    - 7.480177 metric tons
    - 7565.602 kg DAP = 83333.33 kg of sludge * 0.7304 recovery ratio * 0.05717706 kg phosphorus per kg of sludge * (1 / 0.46)
- discount rate: 3 %

Appendix B: Ornstein-Uhlenbeck Price Simulation

$$\delta pg_t = \mu_g(\theta_g - pg_t)\delta t + \sigma_g \delta W_t^g$$

Here the gas prices change δpg_t is represented by a deterministic mean reversion term, with μ_g indicating the speed at which the process returns to the long-run mean θ_g. The random fluctuation stems from a Wiener Process δW_t^g with standard deviation σ_g.

A reformulation with the Euler-Maryama method can be estimated by OLS to retrieve the parameter used in the simulation.

$$p_{t+\delta t} = \underbrace{(1-\mu_i \cdot \delta t)}_{\beta_i} \cdot p_t + \underbrace{\mu_i \cdot \theta_i \cdot \delta t}_{\alpha_i} + \underbrace{\sigma \cdot \sqrt{\delta t} \cdot \varepsilon}_{\xi \text{ iid normally distributed}}$$

$$(\hat{\mu}, \hat{\theta}_\iota) = \left(\frac{1-\widehat{\beta_\iota}}{\delta t}, \frac{\widehat{\alpha_\iota}}{1-\widehat{\beta_\iota}}\right) \; \hat{\sigma} = \sqrt{\frac{\mathrm{Var}\,(\xi)}{\delta t}}$$

Appendix C: Regression

Selection of regression specification

$$\boldsymbol{P}_{t-1} = pg_{t-1} + pd_{t-1} + pf_{t-1} + pg_{t-2} + pd_{t-2} + pf_{t-2} \tag{1}$$

$$\boldsymbol{P}_{t-1} = pg_{t-1} + pd_{t-1} + pf_{t-1} + pg_{t-2} + pd_{t-2} + pf_{t-2} + pg_{t-3} + pd_{t-3} + pf_{t-3} \tag{2}$$

$$\boldsymbol{P}_{t-1} = pg_{t-1} + pd_{t-1} + pf_{t-1} + pg_{t-2} + pd_{t-2} + pf_{t-2} + tt_{t} \tag{3}$$

$$\boldsymbol{P}_{t-1} = pg_{t-1} + pd_{t-1} + pf_{t-1} + pg_{t-2} + pd_{t-2} + pf_{t-2} + pg_{t-1}^{2} + pd_{t-1}^{2} \tag{4}$$

$$\boldsymbol{P}_{t-1} = pg_{t-1} + pd_{t-1} + pf_{t-1} + pg_{t-2} + pd_{t-2} + pf_{t-2} + pg_{t-1}^{2} + pd_{t-1}^{2} + tt_{t} \tag{5}$$

Table A1: Results for Information Criteria: Akaike, Hannan-Quinn, Schwarz-Bayesian, and Final Prediction Error

	(1)	(2)	(3)	(4)	(5)
AIC(n)	10.60	10.59	10.59	10.47	10.47
HQ(n)	10.69	10.71	10.69	10.58	10.59
SC(n)	10.81	10.89	10.83	10.74	10.77
FPE(n)	40326.27	39734.37	39902.43	35239.57	35405.96

Comparison of observed data and simulations

Figures A1 and A2 compare probability distribution functions of the observed data with the simulated prices from all iteration. The figures show that the OUP prices are not very flexible, while the QVAR and the data distributions have multiple peaks. The axis on both distribution is limited by the maximum and minimum value indicating the absence of extreme prices.

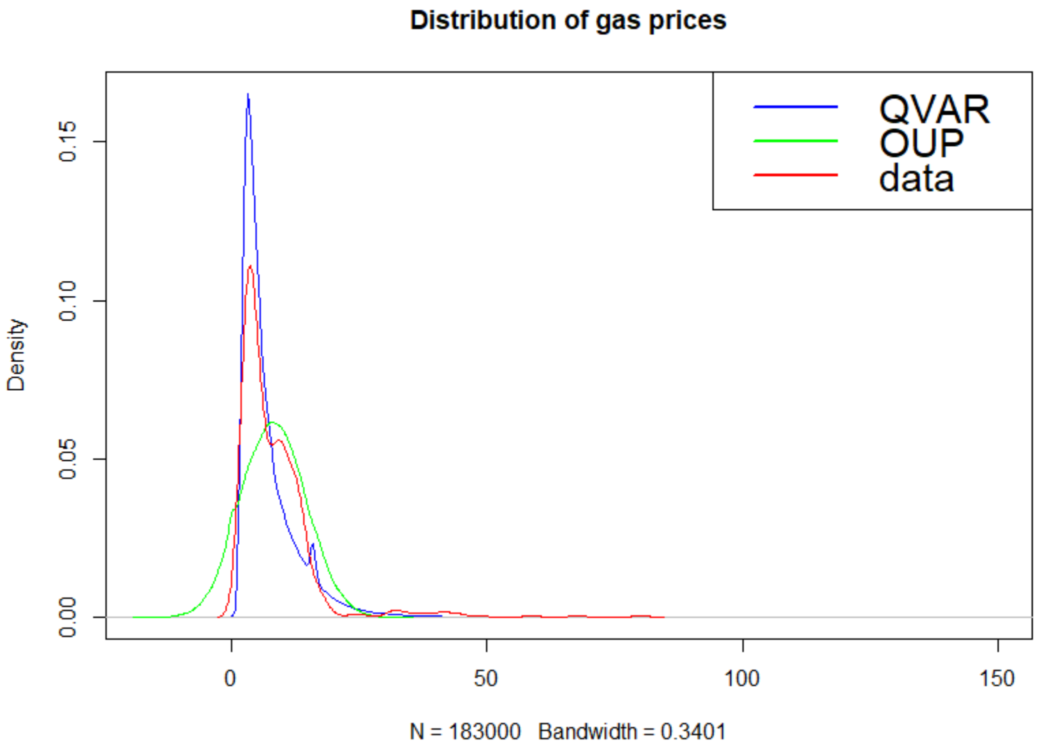

Figure A1: Distribution of gas prices from the observed data and the simulations

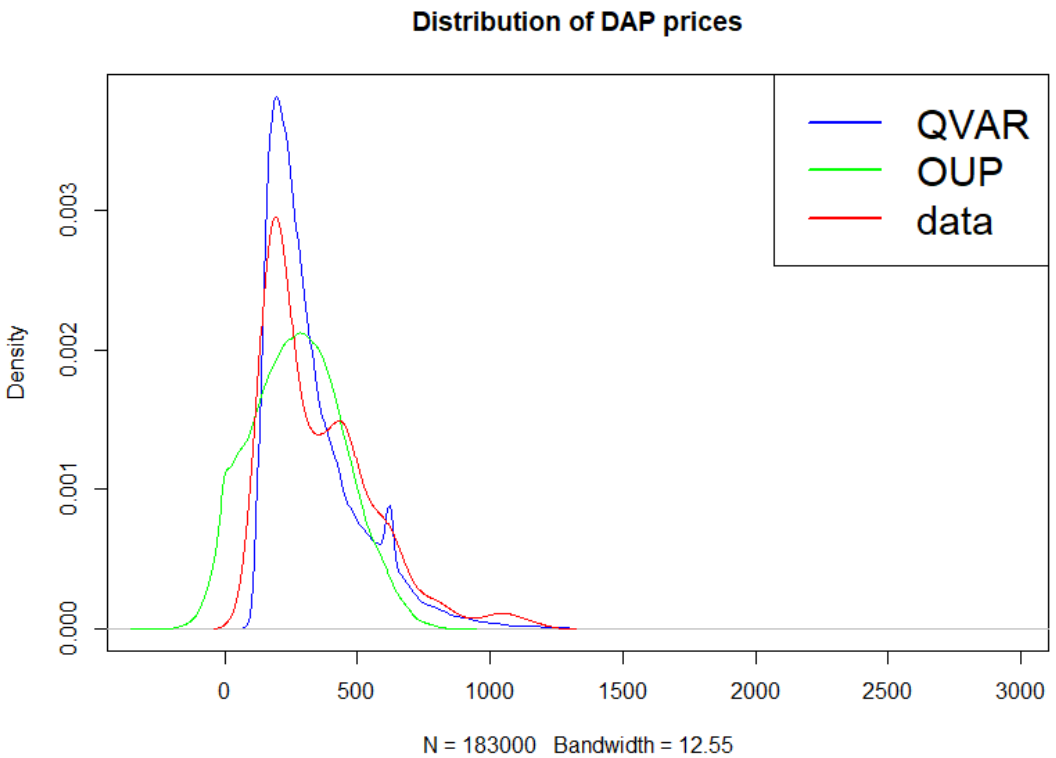

Figure A2: Distribution of DAP prices from the observed data and the simulations

Regression Estimates

The following tables A1-A5 show a selection of the regression results. They contain the results from the VAR estimated by OLS and the quantile regression results for the major quantiles 10, 30, 50, 70 and 90 described in equations (7a-c). Those estimates are in three individual tables each representing different dependent variables gas price, DAP price and the FPI in the (Q)VAR. Moreover, this subsection contains the estimates for the 10, 30, 50, 70 and 90 quantiles of the copula regressions from equation (10 a-b) in tables A5 and A6. The Pseudo-R^2 of the quantile regression is described in Koenker and Machado (1999). Lastly, the tables report the dynamic stability results similar to table 2 in the main manuscript for the 10 and 90 quantiles of the FPI in tables A7 and A8.

Table A2: VAR and QVAR estimates: Gas price equation

	Dependent variable:					
	pg_t					
	OLS	*quantile regression*				
		.1	.3	.5	.7	.9
	(1)	(2)	(3)	(4)	(5)	(6)
pg_1	1.076***	0.753***	0.908***	1.104***	1.222***	1.678***
	(0.049)	(0.216)	(0.115)	(0.048)	(0.164)	(0.150)
pd_1	0.001	0.002	0.003***	0.001	0.002	-0.0005
	(0.004)	(0.004)	(0.001)	(0.001)	(0.002)	(0.003)
pf_1	0.033	0.029	0.018	-0.003	0.002	0.012
	(0.050)	(0.041)	(0.015)	(0.006)	(0.014)	(0.024)
pg_2	-0.214***	-0.123	-0.051	-0.132***	-0.213	-0.475***
	(0.049)	(0.189)	(0.104)	(0.040)	(0.143)	(0.130)
pd_2	0.003	0.002	-0.001	0.00001	-0.001	0.001
	(0.004)	(0.004)	(0.001)	(0.001)	(0.002)	(0.003)
pf_2	-0.117**	0.010	-0.006	0.013**	0.006	-0.001
	(0.051)	(0.045)	(0.015)	(0.006)	(0.015)	(0.025)
Constant	-0.323	0.130	-0.002	0.001	-0.204***	-0.572***
	(0.265)	(0.162)	(0.053)	(0.028)	(0.066)	(0.099)
Observations	404	404	404	404	404	404
R^2	0.911			Pseudo- R^2		
Adjusted R^2	0.910	0.677	0.785	0.837	0.848	0.872

Note: The price lags are denoted by subscript indicating the lag *i* in *t-i*. The quantile regression standard errors are calculated by bootstrapping. The stars denote significance levels of 10 %, 5 % and 1 % as *, **, *** respectively. The Pseudo-R^2 for quantile regression is described in Koenker and Machado (1999).

Table A3: VAR and QVAR estimates: Diammonium Phosphate price equation

	Dependent variable:					
	pd_t					
	OLS	*quantile regression*				
		.1	.3	.5	.7	.9
	(1)	(2)	(3)	(4)	(5)	(6)
pg_1	0.600	0.623	0.260	1.171	0.531	-0.774
	(0.571)	(2.724)	(0.769)	(0.728)	(1.450)	(2.544)
pd_1	1.378***	1.396***	1.358***	1.437***	1.415***	1.338***
	(0.043)	(0.154)	(0.037)	(0.035)	(0.051)	(0.048)
pf_1	0.970*	-0.519	0.120	0.486	1.115***	2.014***
	(0.580)	(1.184)	(0.371)	(0.350)	(0.392)	(0.637)
pg_2	-0.492	-0.124	-0.373	-1.227**	-0.381	1.952
	(0.566)	(2.486)	(0.819)	(0.606)	(1.736)	(2.941)
pd_2	-0.400***	-0.529***	-0.384***	-0.439***	-0.401***	-0.289***
	(0.045)	(0.159)	(0.035)	(0.035)	(0.054)	(0.054)
pf_2	3.439***	0.055	1.546***	1.334***	1.982***	4.243***
	(0.589)	(1.264)	(0.342)	(0.351)	(0.418)	(0.832)
Constant	6.572**	16.022***	3.322**	0.948	0.596	-0.672
	(3.062)	(4.306)	(1.359)	(1.202)	(1.468)	(3.523)
Observations	404	404	404	404	404	404
R^2	0.980	Pseudo- R^2				
Adjusted R^2	0.979	0.805	0.879	0.905	0.907	0.909

Note: The price lags are denoted by subscript indicating the lag *i* in *t-i*. The quantile regression standard errors are calculated by bootstrapping. The stars denote significance levels of 10 %, 5 % and 1 % as *, **, *** respectively. The Pseudo-R^2 for quantile regression is described in Koenker and Machado (1999).

Table A4: VAR and QVAR estimates: Food price index equation

	Dependent variable:					
	pf_t					
	OLS	*quantile regression*				
		.1	.3	.5	.7	.9
	(1)	(2)	(3)	(4)	(5)	(6)
pg_1	0.076	0.170**	0.095*	0.069	0.029	-0.195*
	(0.049)	(0.085)	(0.052)	(0.052)	(0.201)	(0.117)
pd_1	-0.0004	0.012	-0.002	0.002	-0.0003	-0.002
	(0.004)	(0.012)	(0.005)	(0.005)	(0.008)	(0.006)
pf_1	0.370***	0.233***	0.176***	0.319***	0.431***	0.598***
	(0.050)	(0.083)	(0.053)	(0.051)	(0.081)	(0.064)
pg_2	-0.042	-0.055	-0.045	-0.076*	-0.059	0.287**
	(0.049)	(0.073)	(0.073)	(0.043)	(0.252)	(0.141)
pd_2	-0.002	-0.023*	-0.003	-0.002	0.003	0.006
	(0.004)	(0.013)	(0.005)	(0.005)	(0.008)	(0.007)
pf_2	0.063	-0.110	0.019	0.062	0.133	0.089*
	(0.051)	(0.105)	(0.050)	(0.056)	(0.081)	(0.046)
Constant	0.643**	0.125	0.059	0.122	0.570*	0.927***
	(0.265)	(0.416)	(0.216)	(0.195)	(0.302)	(0.157)
Observations	404	404	404	404	404	404
R^2	0.191			Pseudo- R^2		
Adjusted R^2	0.179	0.210	0.094	0.072	0.107	0.233

Note: The price lags are denoted by subscript indicating the lag *i* in *t-i*. The quantile regression standard errors are calculated by bootstrapping. The stars denote significance levels of 10 %, 5 % and 1 % as *, **, *** respectively. The Pseudo-R^2 for quantile regression is described in Koenker and Machado (1999).

Table A5: Quantile estimates: Conditional Gas copula

	Dependent variable:				
			q_g		
	.1	.3	.5	.7	.9
	(1)	(2)	(3)	(4)	(5)
q_f	0.072	0.111	0.143*	0.182**	0.100*
	(0.047)	(0.074)	(0.076)	(0.077)	(0.051)
Constant	0.050*	0.240***	0.403***	0.566***	0.814***
	(0.028)	(0.034)	(0.040)	(0.050)	(0.031)
Observations	403	403	403	403	403

Note: q_d and q_f denote the quantile distribution of DAP and the FPI. The quantile regression standard errors are calculated by bootstrapping. The stars denote significance levels of 10 %, 5 % and 1 % as *, **, *** respectively.

Table A6: Quantile estimates: Conditional DAP copula

	Dependent variable:				
			q_d		
	.1	.3	.5	.7	.9
	(1)	(2)	(3)	(4)	(5)
q_f	0.078	-0.099	-0.073	0.000	0.000
	(0.050)	(0.079)	(0.088)	(0.077)	(0.051)
Constant	0.048*	0.330***	0.510***	0.690***	0.890***
	(0.029)	(0.054)	(0.045)	(0.039)	(0.034)
Observations	403	403	403	403	403

Note: q_d and q_f denote the quantile distribution of DAP and the FPI. The quantile regression standard errors are calculated by bootstrapping. The stars denote significance levels of 10 %, 5 % and 1 % as *, **, *** respectively.

Dynamic stability results for different FPI quantiles

Table A7: Modulus of the dominant root for selected gas and DAP quantiles at the 0.1 quantile FPI

q_d q_g	0.1	0.3	0.5	0.7	0.9
0.1	0.828	0.909	0.947	0.962	0.989
	(0.00184)	(0.00137)	(0.00119)	(0.00143)	(0.00181)
0.3	0.887	0.925	0.956	0.977	1.005
	(0.00148)	(0.001)	(0.00085)	(0.00096)	(0.00133)
0.5	0.958	0.968	0.979	0.997	1.021
	(0.00129)	(0.00092)	(0.00071)	(0.00063)	(9e-04)
0.7	1.02	1.025	1.03	1.046	1.069
	(0.00247)	(0.00233)	(0.00223)	(0.002)	(0.00175)
0.9	1.306	1.307	1.308	1.311	1.316
	(0.00516)	(0.0051)	(0.00506)	(0.0049)	(0.0047)

Note: The table shows the estimated modulus from the dominant root $|\lambda_d|$. The bootstrap standard errors are below in parenthesis. q_d indicates the DAP quantile, q_g indicates the gas quantile.

Table A8: Modulus of the dominant root for selected gas and DAP quantiles at the 0.9 quantile FPI

q_d q_g	0.1	0.3	0.5	0.7	0.9
0.1	0.818	0.943	0.991	1.024	1.074
	(0.00177)	(0.00103)	(0.00055)	(7e-04)	(0.00104)
0.3	0.883	0.946	0.991	1.026	1.077
	(0.0015)	(8e-04)	(5e-04)	(0.00063)	(0.00092)
0.5	0.957	0.971	0.995	1.028	1.077
	(0.00131)	(0.00079)	(0.00048)	(0.00058)	(0.00089)
0.7	1.018	1.023	1.033	1.059	1.101
	(0.00251)	(0.00233)	(0.00215)	(0.00182)	(0.00147)
0.9	1.305	1.305	1.306	1.31	1.317
	(0.00518)	(0.00516)	(0.00509)	(0.00492)	(0.00463)

Note: The table shows the estimated modulus from the dominant root $|\lambda_d|$. The bootstrap standard errors are below in parenthesis. q_d indicates the DAP quantile, q_g indicates the gas quantile.